Kelvin Probe Force Microscopy with attoAFM I

Technical implementation and modes comparison

Ankit Sharma and Balazs Sipos

attocube systems GmbH, 85540 Haar, Germany

Abstract

We describe how the attocube attoAFM I microscope equipped with the Kelvin probe force microscopy (KPFM) upgrade can enable high-resolution imaging of local variations in sample's work function using two acquisition modes. We detail the hardware and software configuration required to implement both amplitude modulation (AM-KPFM) and frequency modulation (FM-KPFM) in the attoAFM I. We conduct an experimental comparison of these KPFM modes using a bilayer moiré structure consisting of graphene and hBN (hexagonal boron nitride), showing that FM-KPFM delivers superior lateral resolution than AM-KPFM. These results illustrate practical trade-offs between sensitivity and lateral resolution, guiding users in selecting the optimal KPFM mode for nanoscale surface-potential mapping.

1. Introduction

KPFM is an advanced AFM-based technique used for exploring the electronic characteristics of nanoscale materials and devices. This technique quantifies the contact potential difference (CPD) by detecting the capacitive electrostatic forces that arise between a conductive AFM probe and the sample.

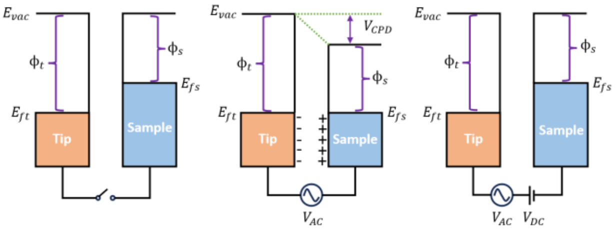

Fig. 1: Working principle of Kelvin probe force microscopy

KPFM utilizes the principles of the Kelvin method [1], which is used to measure the contact potential between a metal probe and a metal sample with dissimilar work functions (ϕ_t and ϕ_s), as illustrated in Figure 1. Initially, in Figure 1a, the two surfaces are brought close together but not connected electrically. At this stage, the work function is defined as the energy required to release a bound electron at the Fermi level (E_f) to the vacuum energy level (E_v). When an electrical connection is established between the distinct metals, electrons flow from the metal with the lower work function to the one with the higher work function and opposite surface charges are formed on the capacitor plates, as shown in Figure 1b. The resulting contact potential difference (CPD) across the plates can be determined by $V_{CPD} = (\phi_t - \phi_s)/e$. Next, to measure the CPD, an external bias voltage (VDC) is applied to either the probe or the sample and adjusted until the surface charges between the probe and sample are nullified. In this equilibrated state, VDC corresponds to the CPD or work function different between different materials, Figure 1c.

The electrostatic force between the cantilever and the sample can be described as:

$$F_{el} = \frac{1}{2}\frac{\partial C}{\partial z}\Delta V^2 \tag{1}$$

Where C is the capacitance between tip and sample at z distance and ΔV refers to the potential difference between the probe and the sample. It is determined by the combination of the intrinsic CPD with the sum of all externally applied voltages to the tip, which includes both the DC voltage (V_{DC}) and the AC voltage (V_{AC}), which can be written as:

$$\Delta V = V_{DC} - V_{CPD} + V_{AC}\,\sin(\omega_e t) \tag{2}$$

The resulting electrostatic force is obtained by substituting equation (1) into (2) and can be divided into one static and two dynamic spectral components.

$$F_{el} = F_{stat.} + F_{\omega_m} + F_{2\omega_m} \tag{3}$$

$$F_{stat.} = \frac{1}{2}\frac{\partial C}{\partial z}(V_{DC} - V_{CPD})^2 + \frac{(V_{AC})^2}{4},$$

$$F_{\omega_m} = \frac{\partial C}{\partial z}\,(V_{DC} - V_{CPD})V_{AC}\,\sin(\omega_m t),$$

$$F_{2\omega_e} = -\frac{\partial C}{\partial z}\,\frac{(V_{AC})^2}{4}\cos(2\omega_m t)$$

The static force component $F_{stat.}$ causes a static bending of the cantilever and do not vary with time. On the other hand, the first and second harmonic electrostatic forces, F_{ω_m} and $F_{2\omega_m}$ are induced by an AC bias at frequency f_m. The amplitude of ω_m component is directly proportional to CPD, while the amplitude of the $2\omega_m$ component is independent of CPD. The KPFM setup is based on the detection and minimization of the ω-component or its gradient by applying a DC voltage to compensate for the CPD.

A Schematic setup of a KPFM is shown in Figure 2. KPFM is performed in non-contact mode at a certain lift height utilizing a conductive tip which is the reference electrode that forms a capacitor with the sample surface. In contrast to MFM or EFM, the cantilever is not mechanically excited at its resonance frequency by using a dither piezo, but it is electrically excited by applying an AC voltage. When there is a direct-current (DC) potential difference between the tip and the surface, the voltage offset will cause the cantilever to vibrate. So, the idea is to minimize the oscillation amplitude by applying a nulling DC bias voltage V_{DC}. The DC voltage to the tip will compensates the AC voltage such that there is no deflection (force) on the cantilever. A map of this nulling DC potential basically gives a KPFM image.

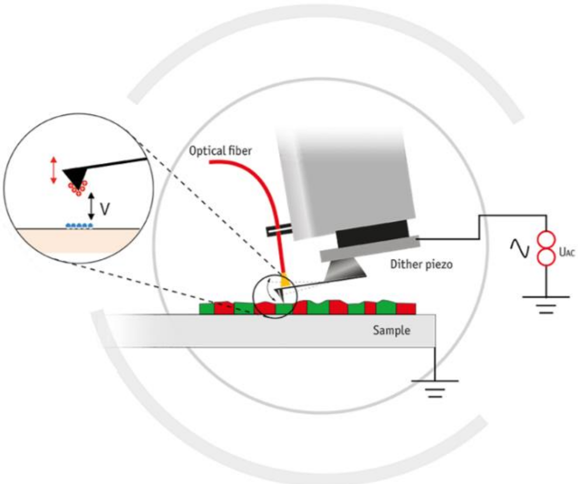

Fig. 2: Schematic diagram of KPFM in attoAFM I microscope.

2. Methods of KPFM

The KPFM can be implemented in two primary acquisition modes: Amplitude modulation (AM-KPFM) and frequency modulation (FM-KPFM), which are sensitive to the electrostatic force and force gradient, respectively. Both modes detect the CPD by applying an AC bias voltage, which modulates the electrostatic force between the tip and sample and results in either a change in cantilever amplitude or resonance frequency. There are different ways to operate these two KPFM modes depending on the selection of the excitation and detection frequencies. An overview of all the KPFM modes in shown in Figure 3.

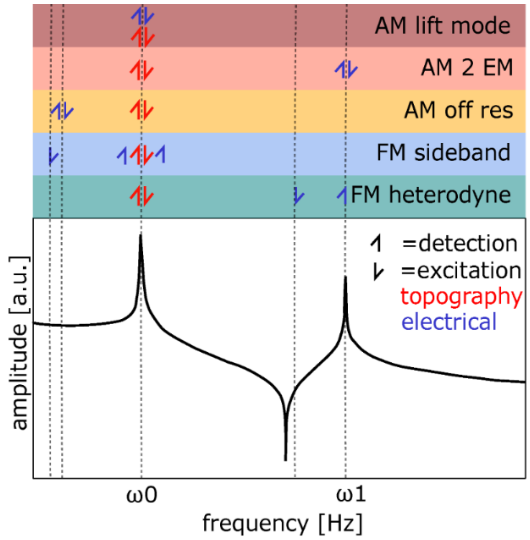

Fig. 3: Overview of KPFM modes. Adapted from [3].

Common to all KPFM modes, however, is the use of closed loop bias feedback, PID controller, adjusting the VDC to nullify electrostatic force ω-component or its gradient and hence determine the CPD. In this study we will focus on implementation of lift mode AM-KPFM and sideband FM-KPFM in AFM I.

2.1. AM-KPFM

AM-KPFM operates by detecting the first harmonic amplitude response A_{ω_m} of the force F_{ω_m} acting on the cantilever. Next, a feedback loop is then utilized to adjust the voltage (V_{DC}) until Aw is nullified, corresponding to $V_{DC} = V_{CPD}$. The output of the KPFM feedback loop, the nulling voltage V_{DC} provides a comprehensive map of the CPD as the tip is systematically scanned across the sample surface. The feedback loop specifically utilizes the in-phase amplitude component (X or quadrature Y) as input, rather than the regular amplitude R. This choice is made because the in-phase component contains crucial information about the phase and polarity of the response.

The electrostatic force is quadratically dependent on the applied voltage and can be measured by the so-called bias spectroscopy as shown in Figure 4. The minimum of amplitude R and zero crossing of in-phase signal X corresponds to the CPD of the sample. The frequency shift signal exhibits a parabolic dependence on the applied DC bias voltage, reaching its maximum at the point where the average electrostatic force is zero, corresponding to the sample's CPD. Thus, the lock-in output, X-component, serves as input to the Kelvin controller which adjusts the V_{DC} such that the oscillation goes to zero.

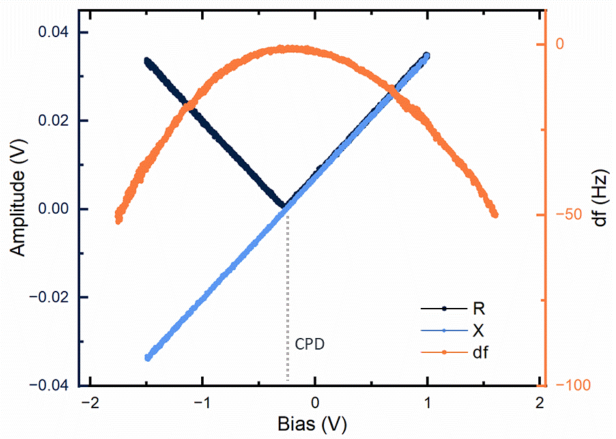

Fig. 4: Open loop bias spectroscopy of lock-in signals (amplitude R and x-component X) and frequency shift as a function of applied bias voltage.

AM-KPFM can be implemented in various ways, depending on the chosen electric excitation frequency f_m. It can be set below the fundamental resonance frequency f_0 or at the first or second eigenmode. Typically, AM-KPFM measurements are performed at the cantilever's resonance frequency to achieve resonant amplification and enhance signal-to-noise ratios.

2.2. FM-KPFM

FM-KPFM operates differently from AM-KPFM as it is sensitive to the electrostatic force gradient rather than the electrostatic force itself. In this technique, the cantilever is mechanically actuated at its resonance frequency while a low-frequency electrical excitation is applied. When an AC-bias voltage is applied, it induces a modulation of the electrostatic force, causing the frequency shift df to oscillate at the AC-bias frequency f_m. A phase locked loop (PLL) is used to detect df and the oscillation is subsequently detected using a lock-in amplifier that is finely tuned to the fm.

In sideband FM-KPFM, a low frequency AC voltage (0.1-1 kHz) is applied to modulate the electrostatic force gradient. The modulated force gradient introduces sidebands at $f_0 \pm f_m$ and $f_0 \pm 2f_m$ adjacent to the fundamental resonance peak at f_0, shown in Figure 5. A feedback loop is then used to nullify the signal at $f_0 \pm f_m$ by applying an appropriate V_{DC}, enabling direct detection of the CPD.

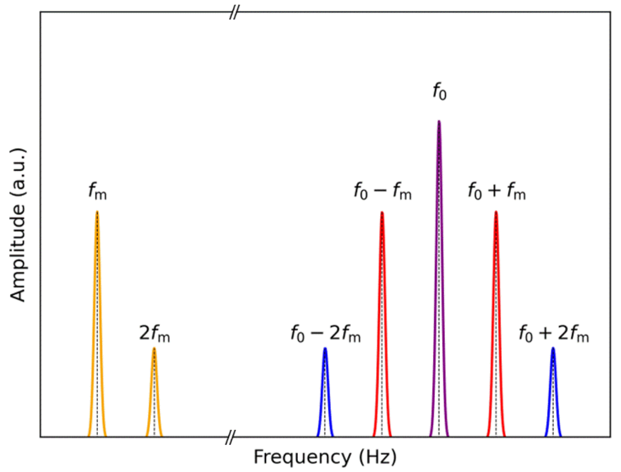

Fig. 5: Schematic representation of the frequency spectrum of the oscillation amplitude in FM-KPFM. sidebands resulting from the frequency modulation induced by the AC bias.

3. AM-KPFM setup

The AM-KPFM setup requires basically the same electronic used for attoAFM I plus an upgrade which enables access to the second lockin mode HF2 in the daisy software. Once KPFM upgrade is enabled, you can switch between the HF channel by selecting the Active HF section 'HF1' or 'HF2' in lever excitation tab.

This also enables the possibility of selecting the lockin modes between ' Amp, phase' (circular coordinate) and 'x, y' (Cartesian coordinate). For dither excitation we always use the circular coordinate; however, for measuring KPFM signal we should use Cartesian coordinate. You could only use one of the two HF channels at the same time, which happens when you change between *Ch1* and *Ch2*. If you select *HF2*, then *HF1* input would be disabled and vice-versa.

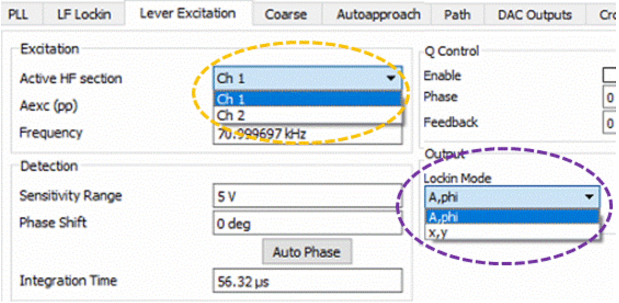

Active HF section: Ch 1
Aexc (pp)
Frequency: 70.999697 kHz
Sensitivity Range: 5 V
Phase Shift: 0 deg
Integration Time: 56.32 µs
Phase: 0
Feedback: 0
Lockin Mode: A,phi

Since *AC* and *DC* voltage are simultaneously applied to the tip, an *AC-DC* coupler serves this purpose. The *HF 2 OUT* connector of the *ASC500* must be connected to the *AC IN* channel of the *AC-DC* module, while the *DAC* channel must be connected to the *DC IN* channel of the *AC-DC* module. The output of the *AC-DC* coupler is connected to the tip.

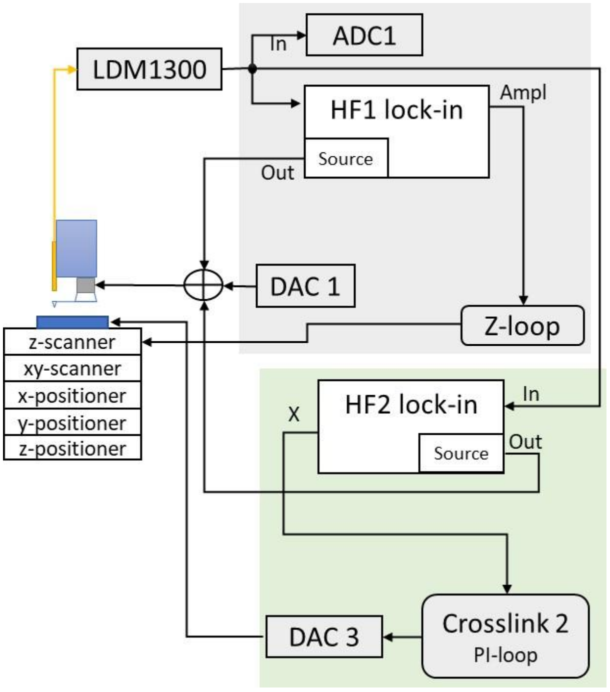

Figure 6: Schematic representation of the signal diagram for AM-KPFM in an AFM I system. The highlighted areas in light grey and green color represent the feedback loops for topography and AM-KPFM, respectively.

To detect the cantilever deflection signal caused by the electrostatic interactions between the sample and the probe, the input signal of *HF-2 lockin*, *HF-In2*, must be connected to *LDM1300* connector (same as *HF-In1* with T-piece BNC).

Thus, the *HF 1* circuit takes care of the physical oscillation of the cantilever via excitation of the dither, while the *HF 2* circuit applies an electric oscillation to the tip. A signal diagram of AM-KPFM is shown in Figure 6.

Once the AM-KPFM setup is ready, the measurements can be performed with the following method.

Constant height mode

The cantilever is piezoelectrically driven at its mechanical resonance frequency using HF-1 and topography of the sample is imaged.

- The cantilever is lifted by a certain height above the sample, and it is electrically excited at the same frequency by giving AC voltage to the tip using *HF-2* in ‘x, y’ lockin mode.
- A spectroscopy of cantilever oscillation amplitude HF 1 x vs *DAC* is taken by sweeping the DC voltage and slope of the zero-crossing line is determined.
- For KPFM scan, the Crosslink functionality is used by selecting one of the Generic Transfer Functions (go to the Crosslink tab). Crosslink will automate the correction of the *HF 1 x* signal by giving a DC voltage to the tip.
- Mapping the Crosslink signal will result in an image of the work function of the sample.

Dual pass mode

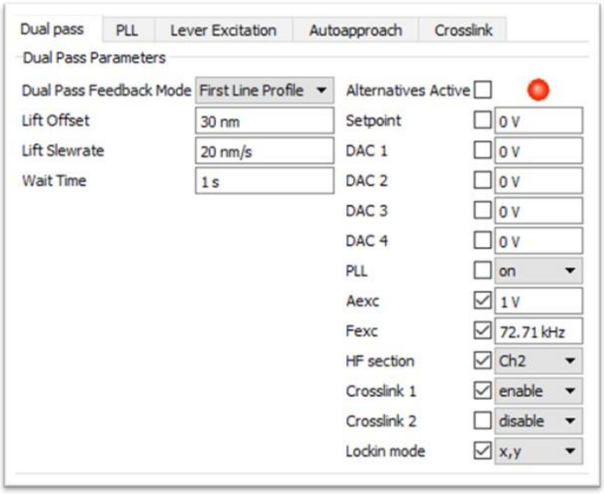

Dual Pass Parameters

Dual Pass Feedback Mode	First Line Profile	Alternatives Active	☐	●
Lift Offset	30 nm	Setpoint	☐	0 V
Lift Slewrate	20 nm/s	DAC 1	☐	0 V
Wait Time	1 s	DAC 2	☐	0 V
		DAC 3	☐	0 V
		DAC 4	☐	0 V
		PLL	☐	on
		Aexc	☑	1 V
		Fexc	☑	72.71 kHz
		HF section	☑	Ch2
		Crosslink 1	☑	enable
		Crosslink 2	☐	disable
		Lockin mode	☑	x,y

- During the first pass, the cantilever is piezoelectrically driven at its mechanical resonance frequency using *HF-1* and topography of the sample is imaged.
- During the second pass, the cantilever is lifted by a desired height and the cantilever is electrically excited using HF-2 channel.
- Go to the Dual Pass tab and pre-configure it with the settings as shown in the image below.

4. FM-KPFM setup

To implement the FM-KPFM measurements, an external Locking amplifier is used to demodulate *df* signal at the electric excitation frequency fm. Here we have used HF2LI lockin amplifier from Zurich Instruments.

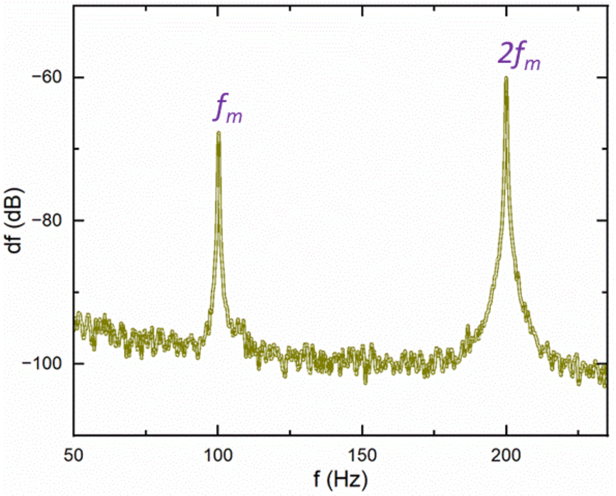

Fig. 7: The frequency shift df exhibits a first and second harmonic frequency component at the electrostatic modulation frequency f_m.

The topography detection is same as for AM-KPFM discussed above i.e., the cantilever is excited at its resonance frequency and the oscillation amplitude *HF Ampl* is used as measuring signal for the z-control feedback loop. The output of z-loop is recorded for topography signal. The AC excitation to the tip is either provided by the LF Lockin of the ASC500 controller or by the signal output of the HF2LI. The demodulated signal Amplitude (from Aux1 of HF2LI) are connected to one of the ADC inputs of the ASC500.

The df signal from the PLL loop and low excitation frequency f_m from LF Lockin are fed into the HF2LI lock-in amplifier. The HF2LI detects the magnitude of the *df* at f_m and gives *X*-component as output after appropriate phase adjustment. This signal serves as input to the Crosslink which automate the correction of the *X*-signal by giving a DC voltage, as shown in Figure 8.

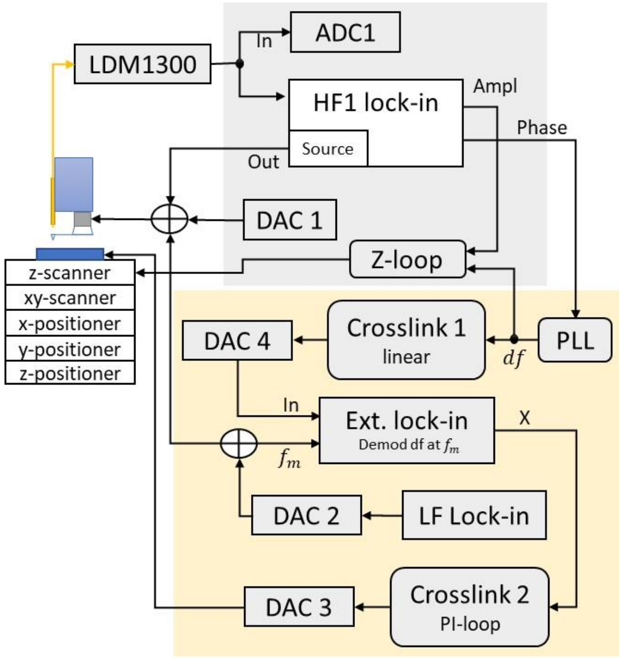

Fig. 8: Schematic representation of the signal diagram for FM-KPFM in an AFM I system. The highlighted areas in light grey and golden color represent the feedback loops for topography and FM-KPFM, respectively.

5. AM-KPFM and FM-KPFM comparison

The utilization of different detection mechanisms in AM-KPFM (electrostatic force) and FM-KPFM (force gradient) within KPFM results in dominant contributions to the signal originating from different regions of the AFM probe.

AM-KPFM can suffer from a reduction in lateral resolution due to the presence of stray capacitance. This stray capacitance arises from the relatively large surface area of the tip cone and cantilever in typical tip/cantilever geometries. Even at short tip-sample distances, which are on the order of a few nanometers, the stray capacitance significantly influences the overall capacitance gradient in the system [4, 5]. Consequently, the stray capacitance effect leads to an averaging of the surface potential over a larger area, diminishing the ability to resolve fine spatial details in the surface potential distribution during AM-KPFM measurements.

By utilizing a frequency-modulated (FM) detection scheme sensitive to electrostatic force gradients, the influence of the long-ranged electrostatic interaction of the cantilever can be minimized [6, 7]. The electrostatic force gradient decays over shorter distances compared to the electrostatic force, resulting in reduced impact from the cone and cantilever on the overall surface potential image. Consequently, FM-KPFM achieves higher spatial resolution by being more sensitive to the electrostatic forces confined to the tip apex, surpassing the capabilities of AM-KPFM [8]. This capability is particularly beneficial for samples with complex topography or materials exhibiting nanoscale surface potential variations. Therefore, FM-KPFM serves as a valuable tool for studying nanoscale electrical properties and mapping surface potential variations with improved accuracy and resolution.

We conducted an experimental comparison of AM-KPFM and FM-KPFM methods using a graphene/hBN sample, Figure 9. The results revealed that sideband FM-KPFM exhibited enhanced spatial and potential resolution compared to AM-KPFM. In sideband FM-KPFM, we observed a CPD contrast of 460 mV, and it effectively resolved small features and edges with high precision. On the other hand, FM-KPFM displayed a CPD difference of 210 mV, indicating lower sensitivity to local potential variations.

Furthermore, FM-KPFM demonstrated blurred edges and features in comparison to the distinct and well-resolved edges captured by sideband FM-KPFM, emphasizing the superior spatial resolution of the latter method. These findings suggest that sideband FM-KPFM offers significant advantages in accurately mapping and characterizing surface potential variations, making it a promising technique for high-resolution nanoscale investigations of different samples.

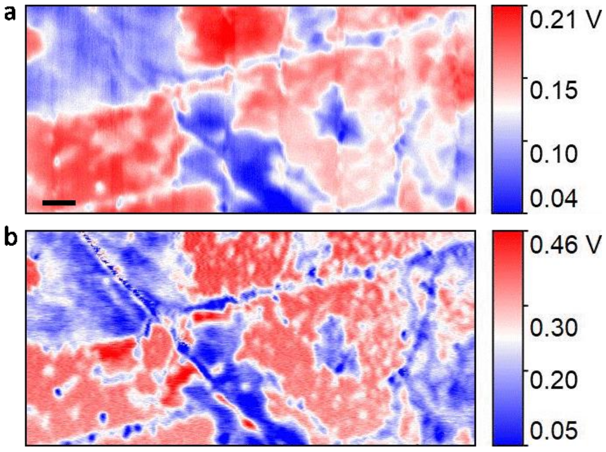

Fig. 9: KPFM image of graphene/hBN. a) AM-KPFM and b) sideband FM-KPFM. The scale is 1 µm.

6. Conclusion

This Note demonstrates the successful implementation of AM-KPFM and FM-KPFM modes on the attocube attoAFM I platform and highlights the practical considerations for each method.

While AM-KPFM offers higher signal sensitivity, its lateral resolution is limited by long-range capacitive contributions from the cantilever and tip cone. In contrast, FM-KPFM minimizes these contributions by sensing the electrostatic force gradient, enabling significantly improved spatial resolution.

However, FM-KPFM also presents trade-offs: it typically requires higher AC bias voltages, which may not be suitable for

some sensitive materials, e.g., in the case of tip-induced band bending on the surface of semiconducting samples [9, 10]. The choice between AM- and FM-KPFM should therefore be guided by the specific experimental requirements, including the desired balance between sensitivity, resolution, measurement speed, and sample compatibility.

By providing a direct comparison of both techniques on a graphene/hBN heterostructure, this work serves as a practical reference to help researchers configure, optimize, and apply KPFM on the attoAFM I system for nanoelectrical studies.

References

[1] L. Kelvin et al., *Contact electricity of metals*. Philos. Mag. **46**, 82 (1898).
[2] S. Saint et al., *Electrostatic forces between metallic tip and semiconductor surfaces*. J. Appl. Phys. **77**, 3308 (1995).
[3] A. Axt et al., *Know your full potential: Quantitative Kelvin probe force microscopy on nanoscale electrical devices*. Beilstein J. Nanotechnol. **9**, 1809 (2018).
[4] H. Jacobs et al., *Resolution and contrast in Kelvin probe force microscopy*. J. Appl. Phys. **84**, 1168 (1998).
[5] T. Wagner et al., *Kelvin probe force microscopy for local characterisation of active nanoelectronic devices*. Beilstein J. Nanotechnol. **6**, 2193 (2015).
[6] D. Ziegler et al., *Force gradient sensitive detection in lift-mode Kelvin probe force microscopy*. Nanotechnology **22**, 075501 (2011).
[7] U. Zerweck et al., *Accuracy and resolution limits of Kelvin probe force microscopy*. Phys. Rev. B **71**, 125424 (2005)
[8] J. Colchero et al., *Resolution enhancement and improved data interpretation in electrostatic force microscopy*. Phys. Rev.B **64**, 245403 (2001).
[9] T. Glatzel et al., *Amplitude or frequency modulation-detection in Kelvin probe force microscopy.* Appl. Surf. Sci, **210**, 84 (2003).
[10] H. Ishii et al., *Kelvin probe study of band bending at organic semiconductor/metal interfaces: examination of Fermi level alignment*. phys. status solidi **201**, 1075 (2004).